INSTRUMENTATION FOR VECTOR ELECTRIC FIELD MEASUREMENTS FROM DE-B

N. C. MAYNARD*, E. A. BIELECKI*, and H. F. BURDICK**
Goddard Space Flight Center. Greenbelt, Maryland 20771, U.S.A.

(Received 20 April, 1981)

Abstract. Instrumentation has been developed using the symmetric double floating probe technique to make vector electric field measurements from the low altitude Dynamics Explorer (DE-B) spacecraft. Six 11 m cylindrical antennas are deployed along 3 orthogonal axes to form the sensor array. The outer two meters of each element are used as sensors which results in a baseline of 21.4 m for the DC measurement for each axis. Efforts have been made to provide straight antennas and antennas that will not bend from thermal stresses as sun angles are changed. Measurements of the DC electric field will be made 16 times per s or every half kilometer along the orbit. Sensitivity will be 0.1 mV m^{-1} with a range of ± 1 V m^{-1}. A 20 channel comb filter spectrometer will monitor AC electric fields, concentrating on frequencies below 1 kHz. Electric fields from any single axis or two axes may be sampled by the spectrometer within the range of 1 μV m^{-1} to 10 mV m^{-1}.

1. Introduction

The general objective of the Dynamics Explorer Program is to investigate the strong interactive processes coupling the hot tenuous convecting plasmas of the magnetosphere and the cooler denser plasmas and gases corotating in the Earth's ionosphere, upper atmosphere and plasmasphere [1]. Primary driving forces for these plasmas come from electric fields and neutral winds. Thus, accurate vector electric field measurements are essential to the understanding of these processes. In this context, the Vector Electric Field Instrument (VEFI) was developed for DE-B to provide large dynamic range, high temporal/spatial resolution, triaxial electric field measurements. Utilizing the short orbit period of the low orbiting DE-B spacecraft, VEFI will monitor the overall framework of the electric field sources as they map to or exist in the ionosphere as well as the detailed structure relative to smaller scale coupling phenomena.

The detailed scientific program objectives have been summarized by Hoffman [1]. Almost all of these involve electric fields in some respect. The DC electric field magnitudes vary from the 1 to 3 mV m^{-1} level generally associated with the ionospheric mid-latitude S_q dynamo [2], to the typically 20 mV m^{-1} electric field seen over the polar cap [3], and to the higher and more variable auroral zone electric fields [3, 4]. Electric fields of over 100 mV m^{-1} are not uncommon in the auroral zone. Recent measurements of 0.5 to 1 V m^{-1} electric fields high above the ionosphere in the 2000 to 5000 km altitude region have been made by the S3-3 satellite [5]. While these large magnitudes are not anticipated over the DE-B orbit, VEFI will have the capability to resolve them.

* Laboratory for Extraterrestrial Physics.
** Space Technology Division.

Space Science Instrumentation **5** (1981) 523–534. 0377–7936/81/0054–0523 $01.80.

Variational or AC electric fields, especially below 1 kHz typically exceed 1 mV m^{-1} RMS in the auroral regions and often reach 0.1 mV m^{-1} at low latitudes when spread F conditions exist [6]. To cover all conditions expected over the DE-B orbit VEFI provides a range of 1 μV m^{-1} to 10 mV m^{-1} RMS.

VEFI uses the double floating probe technique for electric field measurements. A brief description of the technique is given in the next section. In the relatively dense plasmas encountered in the DE-B orbit (compared to those that will be seen near apogee on DE-A), a probe separation of 20 m is adequate for accurate DC measurements. While much has been learned from the single component probe measurements on OGO-6, INJUN-5, and S3-2 [3, 7, 8] and the ion drift measurements on the AE satellites [9], VEFI is expected to provide the first satellite high-resolution triaxial electric field measurements at ionospheric altitudes.

2. The Symmetric Double Floating Probe Technique

The double floating probe technique is a reliable method for direct in situ measurements of electric fields in the plasma medium of the ionosphere and magnetosphere. In view of the numerous past descriptions of this technique in proposals, papers, etc. [10–16], and of the proven flight history on both sounding rockets and satellites [11, 3, 7, 8, 17, 5, 18], only a rudimentary description will be given here and attention will be paid only to technique details pertinent to this mission application.

If no current is drawn from a body in a plasma, its potential will adjust so as to maintain a current balance; therefore this potential will be dependent on the properties of the medium including differences of potential existing in the medium itself. The technique for each vector component is to measure the floating potential of each of two symmetric probes relative to the spacecraft and to subtract these potentials to remove the spacecraft floating potential (see Figure 1). With the existence of an electric field and probe motion it can be shown that

$$(V_A - V_S) - (V_B - V_S) = V_A - V_B = (\mathbf{E} + \mathbf{v} \times \mathbf{B}) \cdot \mathbf{d} \tag{1}$$

where $\mathbf{E}$ is the ambient electric field in the medium, $\mathbf{v}$ is the satellite velocity relative to the inertial system of the plasma, $\mathbf{B}$ is the magnetic field vector, $\mathbf{d}$ is the vector distance between midpoints of the probes (hence, the baseline or gain of the system), and V is the floating potential with the subscript denoting the probe (A or B) or the spacecraft (S). While in the past both spherical and cylindrical probes have been successfully used, cylindrical probes have been chosen for their relative mechanical ease in deployment to long lengths and their smaller perturbation to the spacecraft moment of inertia.

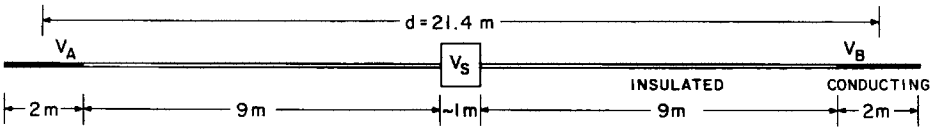

Fig. 1. Double floating probe technique. The dimensions given apply to each of the three axes for VEFI.

In the non-spinning, low altitude DE-B mission the major sources of error in the potential difference measurement arise from contact potential differences and from imprecise knowledge of $\mathbf{v} \times \mathbf{B}$ in spacecraft coordinates, a quantity that must be vectorially subtracted from the measured values to obtain the ambient electric field **E** (see Equation 1). Photo electron emission differences between the sensors will not in general be important since the ambient electron densities are significantly greater; however, when one sensor is shadowed by the spacecraft or when measurements are made under very low density conditions near apogee the data must be evaluated for possible problems. Contact potential differences represent a serious unknown. In the non-spinning situation these differences are not distinguishable from electric fields. By being careful with the sensor surface properties, the contact potential should remain relatively constant over significant time periods (several orbits to days). This allows evaluations of these contact potentials in regions where the ambient electric field is expected to be near zero. The values so obtained are then used over the whole orbit. The $\mathbf{v} \times \mathbf{B}$ induced electric field can be accurately calculated in the inertial system; however, this must be rotated into the spacecraft coordinate system of the sensors in order to perform the vector subtractions. Since $\mathbf{v} \times \mathbf{B}$ may be as much as 450 mV m^{-1}, small uncertainties in the knowledge of the spacecraft attitude or imprecise knowledge of the exact sensor axis will have significant effects on the accuracy of the measurement. Every 0.1° uncertainty in attitude knowledge creates up to a 0.8 mV m^{-1} uncertainty in the measured ambient electric field (note that the actual uncertainty value will vary depending on the magnitude of the above effects).

The parameters that are being measured by the VEFI instrument, their resolution and their range are given in Table I. A brief description of the sensors and electronics which have been designed to perform these measurements is found in the following two sections.

TABLE I

Geophysical parameters

	Range	Amplitude resolution	Temporal/spatial resolution
• Vector DC electric field (3 components)	±1 V m^{-1}	0.1 mV m^{-1}	16 samples s^{-1} (½ km) Optional on 1 axis 32 samples s^{-1} (¼ km)
• Fast variation peak detector	±1 V m^{-1}	10 mV m^{-1}	Programmable: 1, 2 or 4 samples s^{-1} (8, 4 or 2 km)
• Variational electric fields			
Comb filter bank A (8 channels)	4–1024 Hz	1 μV m^{-1}–10 mV m^{-1}	Programmable: 1 Peak and a Avg.
Comb filter bank B (8 channels)	4–1024 Hz	1 μV m^{-1}–10 mV m^{-1}	reading of each channel s^{-1} or 2 readings (Peak or Avg.) of each channel s^{-1} (8 or 4 km)
Comb filter bank C (4 channels)	1.02–512.0 kHz		1 or 2 Avg. readings per sec (8 or 4 km)

The accuracy of the measurements will be a function of many variables and will be evaluated in each individual case. The above paragraph identifies the major sources of error that must be dealt with.

3. Antenna Sensors

Significant advancement of our knowledge of the ionospheric and magnetospheric electric field configurations and their variability requires accurate vector measurements. The position of each antenna sensor axis on the spacecraft and the knowledge of that position in the inertial system is most important in determining the accuracy of the measurements. For this reason special attention was paid to the location, straightness and stability of each deployable antenna.

The deployed VEFI antenna array consists of six 11 m antenna elements deployed along three orthogonal axes of the DE-B spacecraft (Figure 2). Each antenna element is a fully formed cylinder of beryllium copper, 2.86 cm in diam as it exits the deployment mechanism. The outboard two meters of each antenna element serve as the sensors for the instrument (except at high frequencies where capacitive coupling makes the whole

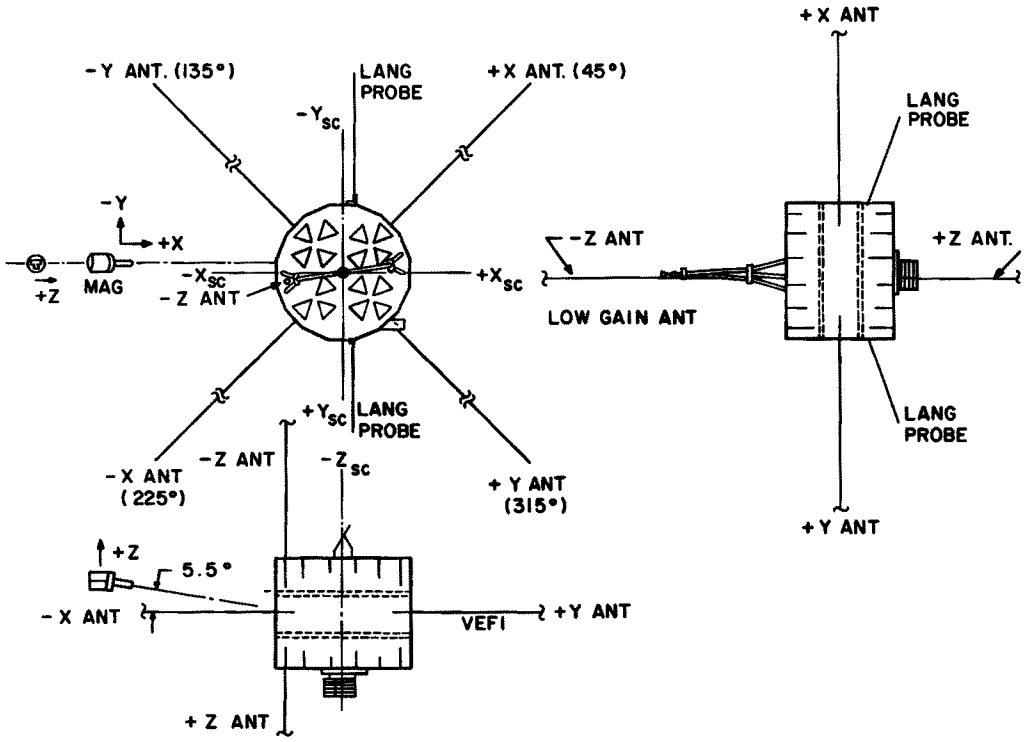

Fig. 2. Schematic of the locations of the three axes of VEFI on the DE-B spacecraft. Note that the electric field axes are rotated about the z axis $-45°$ from the nominal spacecraft axes. The locations of other appendages are shown for reference.

antenna element a sensor). The inboard 9 m of each antenna are covered with a one mil thick insulating film of teflon which is bonded onto the external surface. The insulation provides a separation between the active sensor portion of the element and the spacecraft. This separation is needed to prevent the plasma sheath around the spacecraft from affecting the DC measurements. The dimensional details for each axis are summarized in Figure 1.

In order to minimize antenna warping due to solar heating, the antennas have a highly reflective bright silver coating on the outside surface (under the teflon on the insulated portion), a high absorbtivity black coating on the internal surface, and a random pattern of circular holes (on the inboard 9 m) to permit solar energy to reach the shadowed side and thus reduce temperature differences that cause thermal bending (see Figure 3). The

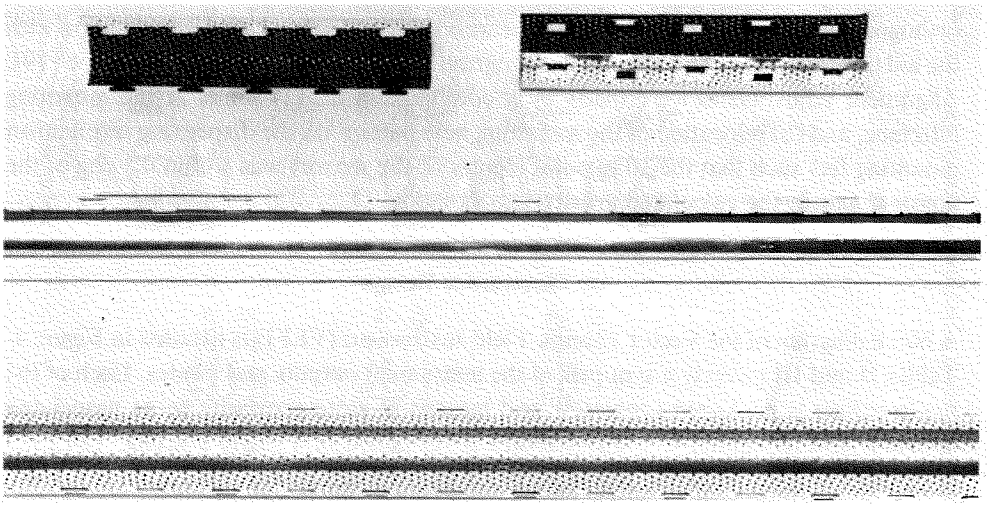

Fig. 3. VEFI antenna element samples. The middle sample shows the silver plated active element. The lower sample shows the insulated portion which is perforated and covered with clear teflon for thermal control. The top sample shows the two halves of element which are locked together with the tabs to form the cylindrical shape. The inside is coated with a black kapton paint as part of the thermal control.

hole pattern was chosen to match the amount of solar energy absorbed by the silver plated front side to that absorbed internally by the black interior and thus provide theoretically no temperature change (hence no thermal bending). The reflective silver plating also provides a noble metal surface on the sensor portion of the element for good electrical coupling to the plasma and stable surface properties.

The tubular antenna element consists of two semicircular shaped strips of beryllium copper joined together by tabs and slots along the edges (see Figure 3). The elements are heat formed into the cylindrical configuration. When retracted into the dispensing mechanism, the antenna is flattened by a series of rollers, and then wrapped and stowed on a spool. The dispensing mechanism is driven by a brushless d.c. motor and gearhead that is reversible for antenna retraction. The moving antenna element drives a roller

which is geared to a 10 turn potentiometer to give an indication of the length of antenna deployed. Mechanically actuated switches cut power to the motor at either full extension or full retraction. Additional switches provide a telemetry signal indicating full deployment and retraction. Electrical contact between the rotating drum to which the antenna element is attached and the RF type connector on the housing is made by a gold plated contact ring in contact with a multiple fingered wiper.

Alignment measurements, which were made to determine antenna element straightness and its orientation with respect to the spacecraft mounting interfaces and the nominal antenna axes, indicated a need to manipulate the antenna dispensing mechanisms in two planes in order to place the active element (centered on the 10 m point) on the reference axis in space. The antennas were suspended vertically for measurements of their shape and orientation in the Optical Test Facility located at the Goddard Space Flight Center. Precise theodolite measurements were taken in two orthogonal planes. These measurements were converted to the gravity free situation with the aid of beam theory and a computer program that plotted the gravity free shape [19]. Alignment adjustments were made by a combination of: (1) shims at the mounting interface, and (b) relocation of the mounting hole pattern on the dispensing mechanism mounting feet such that the 10 m point (center of the sensor) was within 0.1 deg of the nominal axis in the calculated gravity free situation.

4. Electronics Design

A block diagram of the Vector Electric Field Instrument (VEFI) is detailed in Figure 4. Tables II and III provide a synopsis of the instrument outputs and modes. Each of the preamplifiers is packaged separately and located in close proximity to its associated antenna. The remainder of the electronics is contained in a single housing. The total electronics weight, including preamps, is 5.3 kg. Average power dissipation is 7.1 W.

Each preamplifier consists of two high impedance (10^{12} Ω) followers, one DC and one AC, with signal ranges of ± 30 and ± 10 V respectively. The AC follower is a high frequency device whose output is used strictly for analyzing fields above 1 kHz.

The DC outputs of the preamplifiers corresponding to colinear pairs (X, Y, Z) of sensors are accurately subtracted, with the resulting differential signals used as inputs to a 14 bit analog-to-digital converter. Utilizing a track and hold circuit, the differential signals (ΔX, ΔY, ΔZ) are sampled simultaneously and held until processing is complete. Options are provided to also include the common mode voltages (CM), properly scaled, as inputs to the A/D converter via an eight channel multiplexer (See Table II-4). The multiplexer can select any of its eight signals or cycle through the first 2, first 4 or all eight. The input ranges for the differential and common mode voltages are ± 20 and ± 30 V respectively, with corresponding resolutions of 2.44 and 3.66 mV. Therefore, the DC electric field resolution, with a baseline of 21.4 m is 0.114 mV m^{-1}.

The analog-to-digital converter is a 14 bit successive approximation type with an offset binary coded output. Output from the converter is merged with the multiplexed minor mode command verification and instrument status, and is outputed to telemetry as 16

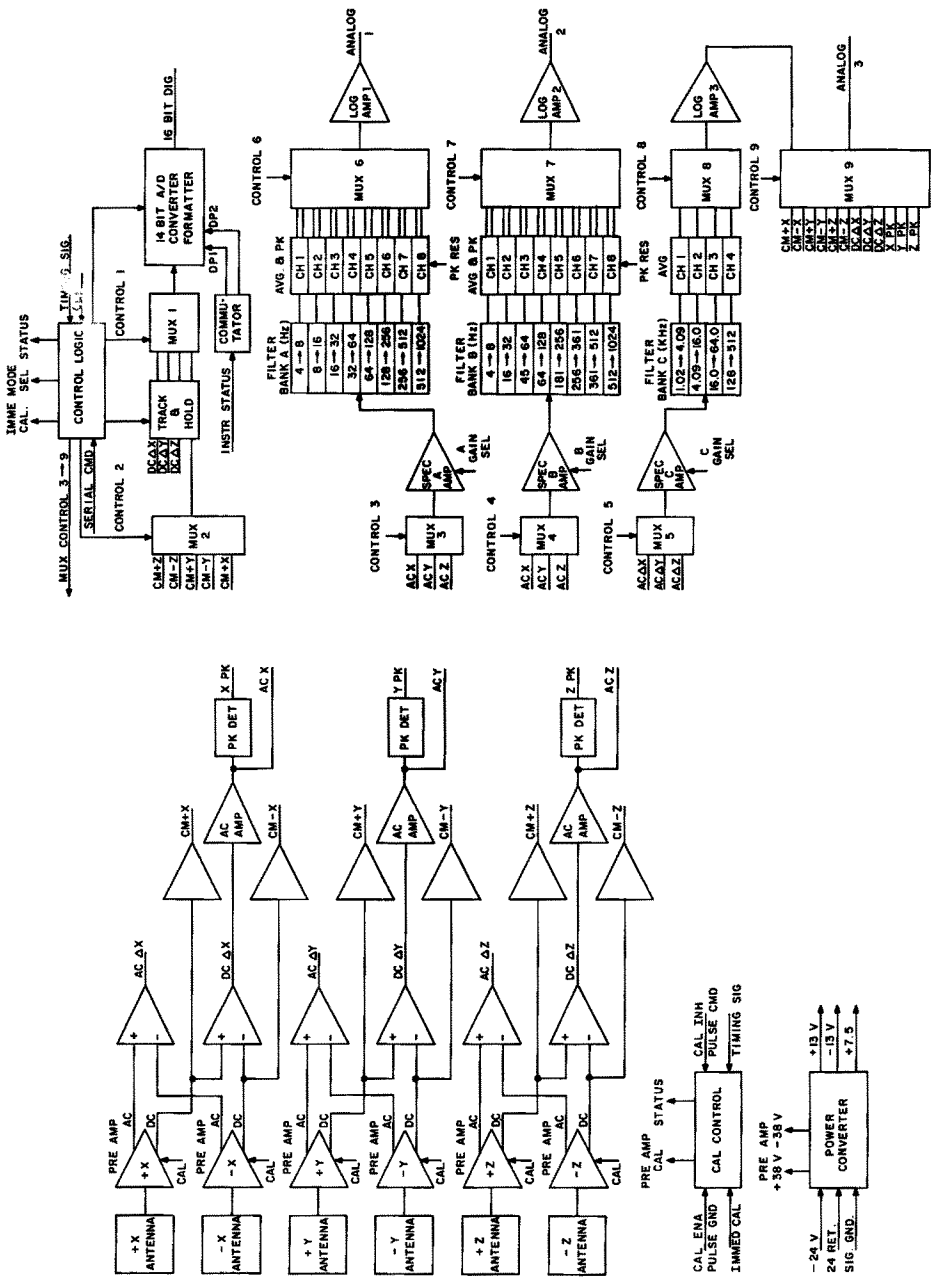

Fig. 4. A block diagram of the VEFI electronics. Each preamp is packaged separately. The remainder of the electronics is packaged together.

TABLE II

Measurements

Four 16 bit digital words (14 bit A/D converter plus 2 status bits)			Samples s^{-1}
1. $\Delta X = V_{+X} - V_{-X}$ (differential)			16
2. $\Delta Y = V_{+Y} - V_{-Y}$ (differential)			16
3. $\Delta Z = V_{+Z} - V_{-Z}$ (differential)			16
4. Programmable (see Table III-5)			16 Fixed input
$CM+Z = V_{+Z} - V_S$ (Common mode)	Alt 2	Alt 4	8 (Alt 2)
$CM-Z = V_{-Z} - V_S$ (Common mode)			4 (Alt 4)
$CM+Y = V_{+Y} - V_S$ (Common mode)			2 (Alt 8)
$CM-Y = V_{-Y} - V_S$ (Common mode)		Alt 8	
$CM+X = V_{+X} - V_S$ (Common mode)			
ΔX			
ΔY			
ΔZ			

8 Bit analog word (multiplexed)

	Samples per s^{-1}	
	Peak or average	Peak and average
Analog 1, spectrometer A, selectable output (see Table III-1)		
5. 4 → 8 Hz	2	1
6. 8 → 16 Hz	2	1
7. 16 → 32 Hz	2	1
8. 32 → 64 Hz	2	1
9. 64 → 128 Hz	2	1
10. 128 → 256 Hz	2	1
11. 256 → 512 Hz	2	1
12. 512 → 1024 Hz	2	1

8 Bit analog word (multiplexed)

	Samples per s^{-1}	
	Peak or average	Peak and average
Analog 2, spectrometer B, selectable output (see Table III-2)		
13. 4 → 8 Hz	2	1
14. 16 → 32 Hz	2	1
15. 45 → 64 Hz	2	1
16. 64 → 128 Hz	2	1
17. 181 → 256 Hz	2	1
18. 256 → 361 Hz	2	1
19. 361 → 512 Hz	2	1
20. 512 → 1024 Hz	2	1

Table II (*Continued*)

8 Bit analog word (multiplexed)

	Samples per s^{-1}			
	Option 1	Option 2	Option 3	Option 4
Analog 3, spectrometer C, selectable output mode (see Table III-3)				
21. 1.02 → 4.09 KHz	2	2	1	1
22. 4.09 → 16.0 KHz	2	2	1	1
23. 16.0 → 64.0 KHz	2	2	1	1
24. 128 → 512 KHz	2	2	1	1
25. X Pk = ΔX peak value	2	1	1	4
26. Y Pk = ΔY peak value	2	1	1	4
27. Z Pk = ΔZ peak value	2	–	1	4

Option 2 includes the common mode voltages at 1 sample s^{-1}.
Option 3 includes both the common mode and differential voltages at 1 sample s^{-1}.

8 Bit 4 second instrument sub-commutator word

	Samples per s^{-1}
Common mode voltages	
28. CM + X	0.5
29. CM − X	0.5
30. CM + Y	0.5
31. CM − Y	0.5
32. CM + Z	0.5
33. CM − Z	0.5

8 Bit spacecraft and instrument sub-commutator words

Preamplifier temperatures, main body electronics temperature, voltage monitor, antenna length monitors, antenna limit flags.

bit data words utilizing two successive 8-bit words. The data sampling rate is four 16 bit words per minor frame corresponding to 16 samples per s for each differential voltage, with an optional 32 samples per s for a given axis by commanding the programmable multiplexer to the differential signal for that axis (See Table II-1 through Table II-4).

The AC portion of the electric field signal is monitored using a twenty channel comb filter spectrum analyzer. This spectrometer is divided into three separate filter banks: two eight channel (A and B) and one four channel (C). Both spectometers A and B cover the range of 4 to 1024 Hz. Spectrometer C covers the frequency range 1 to 512 kHz. All the frequency bands are characterized by a 6th order Butterworth response with the frequencies of the band edges defined at the −6 db points. Spectrometers A and B operate on the DC differential signals while the AC differential signals, derived from the AC outputs of the preamplifiers, serve as inputs to Spectrometer C. The axis to be

TABLE III

Selectable instrument options – serial command

1. Spectrometer A mode select
   a. Input (ΔX, ΔY, or ΔZ)
   b. Gain (low or high)
   c. Output (average and/or peak)

2. Spectrometer B mode select
   a. Input (ΔX, ΔY, or ΔZ)
   b. Gain (low or high)
   c. Output (average and/or peak)

3. Spectrometer C mode select
   a. Input (ACΔX, ACΔY, or ACΔZ)
   b. Gain (low or high)
   c. Output (four options – combinations of spectrometer channels, common mode, differential, and peak voltages)

4. Internal calibration mode select
   a. Cal duration (32 or 64 s)
   b. Cal period (once or twice per orbit)
   c. Immediate calibration
   d. Normal Cal – enable or inhibit

5. A/D Converter input select
   a. Fixed or alternating
   b. Fixed mode – any one of eight inputs selected from the common mode and differential voltages
   c. Alternating mode – three fixed combinations of common mode and/or differential voltages alternating by 2, 4, or 8.

analyzed by each spectrometer is selectable by ground command making it possible to do a fine analysis of one axis or a comparison of any two axes. The outputs of each filter, both average and peak, are compressed logarithmically to cover a range of 70 db. There is no peak detection on the channels in Spectrometer C. Each spectrometer input has an independent gain selectable amplifier. At low gain, Spectrometers A and B cover the RMS range of 5 μV m^{-1} to 9.5 mV m^{-1} while Spectrometer C includes 26 μV m^{-1} to 9.5 mV m^{-1}. At high gain the range covered by Spectrometers A and B is 0.22 μV m^{-1} to 0.44 mV m^{-1} and the range covered by Spectrometer C is 1.3 μV m^{-1} to 0.48 mV m^{-1}. Also included as part of the instrument signal processing is a peak detected output of each of the DC differential signals. The differential signal peak detector outputs, which are multiplexed with the Spectrometer C outputs, will serve as monitors of the DC signal samples in the event of short duration occurrences of electric field transients. The sampling rate for each channel of Spectrometers A and B is 1 sample per s for both peaks and averages and double that for either peaks or averages separately (See Table II-5 through Table II-20). Spectrometer C channels are sampled either once or twice per s and the differential signal peak detector sampling rate is a selectable 1, 2, or 4-samples per s. These and other output options are detailed in Table II-21 through Table II-27 (Options 1, 2, 3, and 4).

Verification of instrument performance is accomplished by an internal calibration sequence occurring normally once or twice per orbit for a duration of either 32 or 64 s. Normal calibration is enabled or inhibited by command and, when desired, immediate calibration can also be commanded. Internal calibration consists of a sequence of DC voltages inputed to each of the six preamplifiers via calibrate relays located in the preamp packages. The relay also disconnects the preamplifiers from the antennas during calibration to minimize perturbing effects.

The power converter design is a conventional two core chopper type operating at 20 kHz. Input conditioning circuitry gives surge current and overvoltage protection and also limits feedback ripple current to a low level. Output regulators are linear dissipative types.

5. Operations

The VEFI has no restrictions on usefulness over the whole DE-B orbit. Thus, it will in general be operated whenever instrument data are being collected. DE is a problem oriented mission; hence each data pass will be oriented toward a particular scientific problem. The instrument modes will be selected to best fit the data to be collected to the problem being attacked. The instrument can be reconfigured with one minor mode command, thus making mode changes within a particular pass operationally feasible.

6. Data Handling and Analysis

All DE data will be processed and analyzed in the DE central computer system as described by Smith *et al.*, [20]. Data will be accessible to all investigators in reduced form through the Mission Analysis Files.

The DC electric field data from VEFI will be converted to geophysical units. Contact potentials, $\mathbf{v} \times \mathbf{B}$ electric fields and co-rotation electric fields will be subtracted from the data to obtain the ambient electric field in coordinate systems corotating with the Earth. The integrated potential along the orbit track will be computed. The $\mathbf{v} \times \mathbf{B}$ electric field will be calculated using either a model magnetic field or the actual measured magnetic field. Contact potential determinations will be done interactively with the DE computer systems. In order to maximize the accuracy of the results it is planned to attempt to calculate the degree of non-orthogonality of the sensor systems from in orbit data and correct for errors so generated. Displays of the DC data will include line and vector plots in linear and polar formats.

The most serious limitation on accuracy will be the knowledge of attitude of the spacecraft. The spacecraft system will provide basically 0.5° attitude knowledge; however, through information from one of the instruments, it is hoped to refine that knowledge to the order of 0.1° [21]. The attitude knowledge is used to transfer the velocity (and calculated **B** if used) into the spacecraft system and to transfer the reduced ambient electric field back from the spacecraft system into topographic or magnetically oriented coordinates.

The AC data will be converted to geophysical units and displayed in line plots and in a gray scale spectrogram format. Specialized analysis work, such as spectral analysis of the DC data, will be done only for specific cases as dictated by the science. A crude approximation of the two DC electric field components in the horizontal plane and AC data in the 8-16 Hz and 4-16 kHz bands will be included in the DE summary plots to aid in the selection of passes for concentrated scientific analysis.

Acknowledgments

We gratefully acknowledge the helpful comments and work of E. Angulo and Dr B. Seidenburg of GSFC on antenna design questions and of Dr J. Fedor of GSFC relative to antenna straightness determinations. The antennas were designed and constructed by Fairchild Industries (Germantown, Md.) under the direction of L. DiBiasi. The electronics were packaged by Ideas, Inc. (Beltsville, Md.). Mr S. W. Billingsley, formerly of GSFC, was responsible for the DC-DC converter and the A-D converter designs. Dr J. P. Heppner is a co-investigator.

References

1. Hoffman, R. A.: *EOS, Trans. Am. Geophys. Union* **61**, 689 (1980).
2. Richmond, A. D., Blanc, M., Emery, B. A., Wand, R. H., Fejer, B. J., Woodman, R. F., Ganguly, S., Ameyenc, P., Behnke, R. A., Calderon, C., and Evans, J. V.: *J. Geophys. Res.* **85**, 4658 (1980).
3. Heppner, J. P.: *Planet. Space Sci.* **20**, 1475 (1972).
4. Maynard, N. C.: *J. Geophys. Res.* **79**, 4620 (1974).
5. Mozer, F. S., Carlson, C. W., Hudson, M. K., Torbut, R. B., Parady, B., Yatteau, J., and Kelley, M. C.: *Phys. Rev. Letters* **38**, 292 (1977).
6. Holtet, J. A., Maynard, N. C., and Heppner, J. P.: *J. Atm. Terr. Phys.* **39**, 247 (1977).
7. Cauffman, D. P., and Gurnett, D. A.: *Space Sci. Rev.* **13**, 369 (1972).
8. Burke, W. J., Hardy, D. A., Rich, F. J., Kelley, M. C., Smiddy, M., Shuman, B., Sagalyn, R. C., Vancour, R. P., Widman, P. J. L., and Lai, S. T.: *J. Geophys. Res.* **85**, 1179 (1980).
9. Heelis, R. A., Winnigham, J. D., Hanson, W. B., and Burch, J. L.: *J. Geophys. Res.* **85**, 3315 (1980).
10. Aggson, T. L. and Heppner, J. P.: 'A Proposal for Electric Field Measurements on ATS-1', Goddard Space Flight Center, Greenbelt, Maryland, 1964.
11. Aggson, T. L.: *Atmospheric Emisions* (B. M. McCormac, ed.), Van Norstrand Reinhold, New York, 1968, p. 305.
12. Fahleson, U. V.: *Space Sci. Rev.* **7**, 283 (1967).
13. Heppner, J. P., Bielecki, E. A., Aggson, T. L., and Maynard, N. C.: *IEEE Trans. Geoscience Electronics* **GE-16**, 253 (1978).
14. Mozer, F. S., Torbert, R. B., Fahleson, U. V., Fälthammar, C.-G., Gonfalone, A., and Pedersen, A.: *IEEE Trans. Geoscience Electronics* **GE-16**, 258 (1978).
15. Mozer, F. S., Cattell, C. A., Temerin, M., Torbert, R. B., VonGlinski, S., Woldorff, M., and Wygant, J.: *J. Geophys. Res.* **84**, 5875 (1979).
16. Burke, W. J., Hardy, D. A., Rich, F. J., Kelley, M. C., Smiddy, M., Shuman, B., Sagalyn, R. C., Vancour, R. P., Widman, P. J. L., Lai, S. T., and Bass, J.: 'Report AFGL-TR-79-0011 Air Force Geophysics Laboratory', Bedford, Massachusetts, 1979.
17. Maynard, N. C., Evans, D. S., Maehlum, B., and Egeland, A.: *J. Geophys. Res.* **82**, 2227 (1977).
18. Heppner, J. P., Maynard, N. C., and Aggson, T. L.: *Space Sci. Rev.* **22**, 777 (1978).
19. Fedor, J. V.: 'Report X-712-80-27', Goddard Space Flight Center, Greenbelt, Maryland, 1980.
20. Smith, Paul H., Freeman, Clyde H., and Hoffman, R. A.: *Space Sci. Instrument.* **5**, 561 (1981) (this issue).
21. Hays, P. B., Killeen, T. L., and Kennedy, B. C.: *Space Sci. Instrument.* **5**, 395 (1981) (this issue).